



## Structure-activity relationships of fluorene compounds inhibiting HCV variants

Hee Sun Kim<sup>b,1</sup>, Youngsu You<sup>c,1</sup>, Jaegon Mun<sup>a</sup>, Changdev G. Gadhe<sup>d</sup>, Heejo Moon<sup>c</sup>,  
Jae Seung Lee<sup>b</sup>, Ae Nim Pae<sup>d</sup>, Michinori Kohara<sup>e</sup>, Gyochang Keum<sup>d</sup>, Byeong Moon Kim<sup>c,\*\*</sup>,  
Sung Key Jang<sup>a,b,\*</sup>

<sup>a</sup> Department of Life Sciences, Pohang University of Science and Technology, Pohang, 37673, South Korea

<sup>b</sup> Division of Integrative Biosciences and Biotechnology, Pohang University of Science and Technology, Pohang, 37673, South Korea

<sup>c</sup> Department of Chemistry, College of Natural Sciences, Seoul National University, Seoul, 08826, South Korea

<sup>d</sup> Center for Neuro-Medicine, Brain Science Institute, Korea Institute of Science and Technology (KIST), Seoul, 97270, South Korea

<sup>e</sup> Department of Microbiology and Cell Biology, Tokyo Metropolitan Institute of Medical Science, Tokyo, 156-8506, Japan

### ARTICLE INFO

#### Keywords:

Hepatitis c virus  
Direct-acting antiviral agent (DAA)  
NS5A inhibitor  
Resistance-associated variant (RAV)  
Structure-activity relationship (SAR)  
Molecular docking

### ABSTRACT

Approximately 71 million people suffer from hepatitis C virus (HCV) infection worldwide. Persistent HCV infection causes liver diseases such as chronic hepatitis, liver cirrhosis, and hepatocellular carcinoma, resulting in approximately 400,000 deaths annually. Effective direct-acting antiviral agents (DAAs) have been developed and are currently used for HCV treatment targeting the following three proteins: NS3/4A proteinase that cleaves the HCV polyprotein into various functional proteins, RNA-dependent RNA polymerase (designated as NS5B), and NS5A, which is required for the formation of double membrane vesicles serving as RNA replication organelles. At least one compound inhibiting NS5A is included in current HCV treatment regimens due to the high efficacy and low toxicity of drugs targeting NS5A. Here we report fluorene compounds showing strong inhibitory effects on GT 1b and 3a of HCV. Moreover, some compounds were effective against resistance-associated variants to DAAs. The structure-activity relationships of the compounds were analyzed. Furthermore, we investigated the molecular bases of the inhibitory activities of some compounds by the molecular docking method.

### 1. Introduction

About 71 million people are infected with Hepatitis C virus (HCV) worldwide, causing approximately 400,000 deaths each year. Chronic HCV infection is a major causative agent of chronic hepatitis, liver cirrhosis, and hepatocellular carcinoma (HCC) (Khullar and Firpi, 2015). HCV is an enveloped RNA virus of the *Flaviviridae* family, comprising of a 9.6 kb (+)-sense single strand RNA. To date, the HCV strain has been classified into seven genotypes (GTs) and about 70 subtypes. According to recent estimation, genotype (GT) 1 is the most prevalent (46.2%), followed by GT 3 (30.1%) (Messina et al., 2015). Even though pegylated interferon- $\alpha$  (pegIFN- $\alpha$ ) combined with ribavirin was previously the most commonly used treatment, combinations of direct-acting antiviral agents (DAAs) against HCV are currently the standard for HCV therapy (Zhang et al., 2016). The major targets of

DAAs are NS3/4A protease, NS5B RNA-dependent RNA polymerase, and NS5A (which participates in viral genome replication and encapsidation) (Pietschmann and Brown, 2019). This study focused on the development of anti-HCV compounds targeting NS5A.

NS5A of HCV is a multi-functional protein participating in viral RNA replication, virus assembly, and virion particle release. It also influences many cellular processes such as apoptosis, stress-responses, immune responses, and cell cycle, although no enzymatic activity of NS5A has been reported (He et al., 2006; Huang et al., 2007). NS5A, composed of 450 amino acids, consists of an amphipathic alpha helix region (AH) at the N-terminus, followed by three domains I, II, and III. However, a recent study conjectured that the domains II and III are not clearly distinct as previously suggested (Badillo et al., 2017). Four X-ray crystal structures of the NS5A domain I, excluding the AH region, have been reported (Lambert et al., 2014; Love et al., 2009; Tellinghuisen

\* Corresponding author. , Rm278, POSTECH Biotech Center (PBC), Pohang University of Science and Technology (POSTECH), 77 Cheongam-ro, Nam-Gu, Pohang-si, Gyeongsangbuk-do, 37673, South Korea.

\*\* Corresponding author.

E-mail addresses: [kimbm@snu.ac.kr](mailto:kimbm@snu.ac.kr) (B.M. Kim), [sungkey@postech.ac.kr](mailto:sungkey@postech.ac.kr) (S.K. Jang).

<sup>1</sup> These authors contributed equally to this work.

et al., 2005), and the structure of the AH region was separately determined by NMR (Penin et al., 2004). However, the three-dimensional structure of the full-length NS5A domain I, including the AH region, has yet to be reported.

Sequence analyses of drug resistant variants revealed two regions in NS5A that affect the activity of NS5A inhibitors (Fridell et al., 2010; Sorbo et al., 2018; Teraoka et al., 2018). The first region is near amino acid 31 of NS5A, which corresponds to the flexible linker between the AH region and the rigidly structured core region of domain I. Various changes around this region contribute to drug resistance. However, it is unclear how anti-HCV compounds associate with NS5A since the structure of this flexible linker region is unknown, and the structure of an NS5A-drug complex has never been solved (Lambert et al., 2014; Love et al., 2009; Tellinghuisen et al., 2005). The second region is near amino acid 93 of NS5A within the rigid core of domain I. Four different structures of the rigid core of domain I have been reported. Its overall folding structure was similar in all reports and predicted as dimeric forms. However, the reported contacting regions of the domain I dimers differed from each other (Lambert et al., 2014; Love et al., 2009; Tellinghuisen et al., 2005). Therefore, it is unclear which dimer form of NS5A functions in HCV replication and/or viral particle assembly in cells, providing an additional difficulty in predicting the binding site(s) of anti-HCV drugs targeting NS5A.

Anti-HCV drugs targeting NS5A are highly effective and well tolerated. However, NS5A inhibitors usually have a low genetic barrier for resistance-associated variants (RAVs) development in single compound treatment conditions (Lawitz et al., 2016). We previously reported new anti-HCV compounds targeting NS5A (Bae et al., 2015). Among them, compound **43** containing a 9,9-difluoro-substituted fluorene skeleton showed a very high inhibitory effect on wild type and daclatasvir-resistant mutant L31V (Leu31Val) of GT 1b HCV (Bae et al., 2015). However, it was not highly effective against the major daclatasvir-resistant mutant Y93H (Tyr93His) or double mutant L31V+Y93H (Table 1). Here, we report a new series of NS5A inhibitors containing a fluorene proline-amide skeleton showing strong inhibitory effects not only on both GT 1b and 3a HCV, but also on daclatasvir-resistant mutants. Moreover, the NS5A inhibitors showed low cytotoxicity. Finally, we describe structure-activity relationships (SAR) between the inhibitors and drug resistance mutants through *in vitro* efficacy tests and *in silico* docking studies.

## 2. Materials and methods

### 2.1. Compounds

Testing compounds were synthesized as previously described (Bae et al., 2015; Hee Sun Kim, March, 2019). The synthesized compound was dissolved in dimethyl sulfoxide (DMSO) at a concentration of 10 mM. MK-5172 (grazoprevir) and GS5816 (velpatasvir) were purchased from Shanghai Heat-biochem, BMS-790052 (daclatasvir) and

Geneticin (G418) were purchased from Selleckchem, and AG Scientific, respectively.

### 2.2. Analysis of the compound structure and purity

HPLC analyses were carried out using an Agilent HP1100 system (Santa Clara, CA, USA), composed of an auto sampler, quaternary pump, photodiode array detector (DAD), and HP Chemstation software. The separation was carried out on a poroshell 120 EC-C18 column 50 × 4.6 mm, 2.7 mm with acetonitrile (A), 0.1% TFA in water (B), as a mobile phase at a flow rate of 1 ml/min at 20 °C. Method: 5% A and 95% B (0 min), 50% A and 50% B (15 min), 95% A and 5% B (24 min), 95% A and 5% B (25 min), 5% A and 95% B (26 min), 5% A and 95% B (27 min). All materials were purchased from commercial suppliers and used without further purification unless otherwise noted (Fig. S1).

### 2.3. Construction of plasmids and *in vitro* transcription of RNA

Plasmid pNK5.1-Gluc was constructed by inserting the *Gaussia* luciferase (Gluc) gene into plasmid pNK5.1/Con1 (Krieger et al., 2001). To construct pNK5.1-Gluc, we generated a new *AscI* restriction enzyme site between the HCV IRES and neomycin phosphotransferase region of pNK5.1 by site-directed mutagenesis. A DNA fragment containing the 2A protease gene of foot-and-mouth-disease virus (FMDV) at both N- and C-terminal sides of the *Gaussia* luciferase gene was amplified by PCR. The amplified 2A-Gluc-2A DNA fragment containing *AscI* sites at both ends was digested with the *AscI* enzyme and ligated into the pNK5.1 containing *AscI* site (Fig. 1A). Plasmids encoding GT 1b replicons with drug-resistant mutations (L31V, Y93H, and L31V+Y93H) in NS5A were generated by site-directed mutagenesis using pNK5.1-Gluc as a template.

Plasmid pJC1-Gluc was constructed by inserting the 2A-Gluc-2A DNA fragment between the P7 and NS2 region of pJC1 (Phan et al., 2009; Pietschmann et al., 2006). A new *AscI* restriction enzyme site was inserted between the P7 and NS2 region of pJC1 by site-directed mutagenesis. The 2A-Gluc-2A DNA was digested using the *AscI* enzyme and ligated into the *AscI* site-containing pJC1 (Fig. 1A). Plasmid pS52-Feo, encoding the GT 3a subgenomic replicon, was kindly provided by Dr. Charles M. Rice (The Rockefeller university) (Saeed et al., 2012).

To synthesize GT 1b replicon RNA, *in vitro* transcription was performed using T7 polymerase with *ScaI*-linearized pNK5.1-Gluc DNA. To synthesize GT 2a infectious RNA, *in vitro* transcription was performed using T7 polymerase with *XbaI*-linearized pJC1-Gluc. To synthesize GT 3a replicon RNA, *in vitro* transcription was performed using T7 polymerase with pS52-Feo linearized by *XbaI*.

### 2.4. Cell lines and cell culture

Huh 7.5.1 cells were cultured in Dulbecco's Modified Eagle's medium (DMEM, Gibco™) containing antibiotics (100 U/ml penicillin and 10 µg/ml streptomycin) supplemented with 10% fetal bovine serum (FBS, PEAK, Inc.) in a humidified 6.0% CO<sub>2</sub> incubator at 37 °C. Huh 7.5.1 cells containing a bicistronic HCV replicon NK5.1-Gluc (GT 1b) and S52-Feo (GT 3a) were used to test the anti-HCV activities of chemicals (Fig. 1A). Replicon RNA (30 µg) was transfected into Huh7.5.1 cells. The cells were cultured in DMEM with G418 (0.5 mg/ml, Calbiochem) for selective cultivation of cells containing the HCV replicon. After selection, replicon-containing cells were cultured in DMEM containing antibiotics (100 U/ml penicillin, 10 µg/ml streptomycin, and 0.5 mg/ml G418) supplemented with 10% FBS (PEAK, Inc.).

### 2.5. Virus production

*In vitro* transcribed HCV RNAs were electrophorated into Huh 7.5.1 cells as described previously (Kim et al., 2011). The transfected cells were cultured for 3 days. Following, the culture media containing

**Table 1**  
Effects of compound 43 on various HCV replicons.

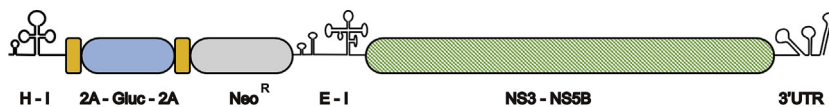
	EC <sub>50</sub> (nM) <sup>a</sup>
GT 1b (NK5.1)	0.003
GT 2a (Jc1)	0.059
GT 3a (S52)	0.014
GT 1b L31V	0.12
GT 1b Y93H	2.3
GT 1b L31V+Y93H	> 1,000
CC <sub>50</sub> <sup>b</sup>	> 20,000

<sup>a</sup> The values depict mean and standard deviation. EC<sub>50</sub>, Effective concentration 50%.

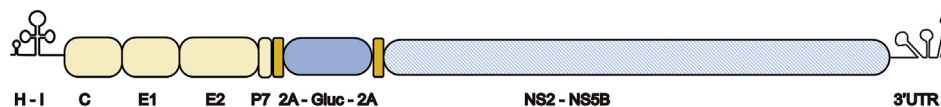
<sup>b</sup> CC<sub>50</sub>, Cytotoxicity concentration 50%. Results from three independent experiments in duplicate.

**A**

Genotype 1b (NK5.1-Gluc)



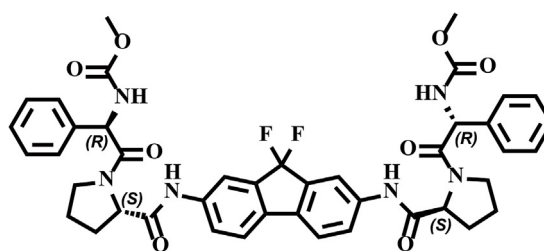
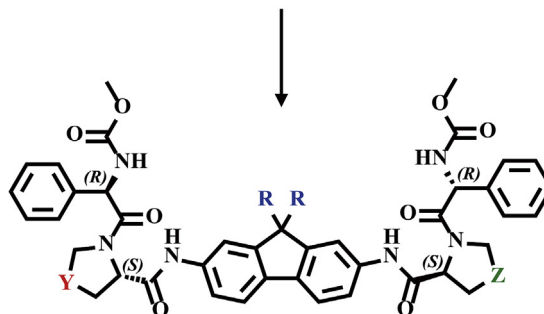
Genotype 2a (Jc1-Gluc)



Genotype 3a (S52-Feo)



- H-I: HCV IRES
- E-I: EMCV IRES
- 2A: FMDV 2A protease
- Gluc: *Gaussia* luciferase
- Fluc: *Firefly* luciferase

**B****Compound 43**

**Fig. 1.** Assay systems to investigate anti-HCV activities of compounds and molecular structure of compound 43 and its modification sites. (A) Schematic diagrams of subgenomic replicons NK5.1-Gluc and S52-Feo, and an infectious HCV clone Jc1-Gluc for testing anti-HCV activities of compounds against GT 1b, 3a, and 2a HCVs, respectively. (B) Molecular structure of compound 43 (upper panel). Modifications of compound 43 at several sites (designated as R, Y, and Z) were executed to develop compounds having higher activities to GT 3 HCV and RAVs of HCV.

virion particles (HCVcc) were collected for 7 days and filtered through a 0.45  $\mu\text{m}$  pore size filter.

## 2.6. Measurement of anti-HCV activities of compounds using HCVcc

Huh 7.5.1 cells were inoculated with JCl1-Gluc virus (Kim et al., 2011; Pietschmann et al., 2006). Four hours after viral inoculation, HCV-infected Huh 7.5.1 cells were cultured with media containing serially diluted inhibitors. Three days post-chemical treatment, culture media were harvested, and *Gussia* luciferase activities in the media were measured using a *Renilla* luciferase assay system (Promega) according to the manufacturer's protocol. Luciferase activities were normalized to those obtained from mock-treated (0.1% DMSO) cells. Further, a four-parameter logistic calculation was used to calculate  $\text{EC}_{50}$  and statistical values in the SigmaPlot Program software (Systat Software Inc.).

## 2.7. Measurement of anti-HCV activities of compounds using HCV replicon

Replicon-containing cells were seeded on a 12-well plate ( $5 \times 10^4$  cells per well). One day after cell seeding, culture media were changed with fresh media containing serially diluted compounds. The cells were further cultured for 3 days. Following, culture media were collected to measure activity of *Gussia* luciferase secreted from cells containing NK5.1-Gluc replicon. *Gussia* luciferase activity was measured using a *Renilla* luciferase assay system (Promega). To measure firefly luciferase activity in cells containing S52-Feo replicon, cells were harvested and lysed after compound treatments for 3 day. Firefly luciferase activities in cell lysates were measured by a firefly luciferase assay system (Promega) according to the manufacturer's protocol. The luciferase activities were normalized to those obtained from mock-treated (0.1% DMSO) cells. Further, a four-parameter logistic calculation was used to calculate  $\text{EC}_{50}$  and statistical values in the SigmaPlot Program software (Systat Software Inc.).

## 2.8. Colony formation assay

Huh 7.5.1 cells containing a HCV replicon (NK5.1-Gluc or S52-Feo) were used for colony formation assays. Replicon-containing cells were seeded on a 6-well plate ( $5 \times 10^4$  cells per well). At 16 h after cell seeding, culture media were changed with fresh media containing serially diluted compounds without G418. The cells were cultured for 5 days. Subsequently, the cells were split into new 6-well plates to about 20% confluence. The cells were further cultured for 5 days and split into new 6-well plates to about 20% confluence. Culture media were changed with DMEM containing 1 mg/ml G418, refreshing every 2–3 days. Two weeks after selection initiation, cells were stained with Crystal violet solution (1% formaldehyde, 1% methanol, and 0.5 g Crystal violet) for 20 min and washed with PBS. Images were captured by an Amersham™ Imager 600 (GE healthcare) following plate drying.

## 2.9. Sequencing of replicon RNAs

After colony formation, total RNAs were isolated from cells using TRIzol reagent (Invitrogen). cDNAs were synthesized using a reverse transcriptase (Promega), and the DNA fragments corresponding to HCV NS5A were amplified by PCR with a pair of primers (forward primer: 5'-GGTACCAGCGGCGATTGGCTGCG-3', reverse primer: 5'-TCTAGAGCAGCAGACCAGCTCT-3'). The amplified DNA fragments were inserted into pcDNA 3.1 vector (Invitrogen) and transformed into *E. coli*. After sequencing the inserted DNAs, the sequences were analyzed by DS gene program.

## 2.10. Cytotoxicity test

Compound cytotoxicity was assessed using a ToxiLight™ (Lonza)

cytotoxicity assay kit, according to the manufacturer's protocol. In brief, Huh 7.5.1 cells were seeded on 24-wells plate ( $2 \times 10^4$  cells per well). One day after cell seeding, culture media were changed with fresh DMEM containing serially diluted compounds. The cells were further cultured for 3 days. Following, culture media were collected and centrifuged to remove cell debris (12,000 rpm, 4 °C, 10 min). Finally, cytotoxicity level was measured by a luminescence reader (Victor 3, Perkin Elmer™) using a ToxiLight™ kit.

## 2.11. hERG ligand binding assay

The hERG ligand binding assay was performed using a Predictor™ hERG fluorescence polarization assay kit (cat no. PV5365) according to the manufacturer's directions. In brief, 5  $\mu\text{l}$  of test compound, 10  $\mu\text{l}$  of membrane, and 5  $\mu\text{l}$  of tracer were applied to a 384-well plate. The plate was covered with aluminum foil to block light and incubated for 2–3 h at room temperature. Fluorescence polarization of the hERG red tracer was measured using a TECAN plate reader (Infinite M1000 pro).

## 2.12. Cytochrome P450 (CYP) inhibition assay




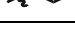
Testing compounds (10  $\mu\text{M}$ ) were incubated with human liver microsomes (0.25 mg/ml) and probe substrate cocktail [Phenacetin (50  $\mu\text{M}$ ), Diclofenac (10  $\mu\text{M}$ ), S-mephenytoin (100  $\mu\text{M}$ ), Dextromethorphan (5  $\mu\text{M}$ ), and Midazolam (2.5  $\mu\text{M}$ )] in 0.1 M phosphate buffer for 5 min at 37 °C. The probe substrates were used to determine activities of CYP1A2, CYP2C9, CYP2C19, CYP2D6, and CYP3A4, respectively. NADPH generation solution was added to the mixtures and further incubated for 15 min at 37 °C. The reactions were stopped by adding acetonitrile. The reaction products were centrifuged at 14,000 rpm for 5 min at 4 °C. Following, the supernatants were injected into a LC-MS/MS system (Shimadzu Nexera XR system and TSQ vantage (Thermo)). Finally, amounts of remaining probe substrates were measured by LS-MS/MS analyses.

## 2.13. Molecular modeling

Two three-dimensional structures of HCV NS5A domain I were downloaded from protein data bank (PDB) as open (PDB code: 1ZH1) and closed (PDB code: 3FQQ) forms (Love et al., 2009; Tellinghuisen et al., 2005). Since both open and closed forms of NS5A structures do not contain information on the N-terminal 1–31 amino acid residues that are likely to participate in association with anti-HCV compounds, we modeled the missing component (UniProtKB = Q9WMX2) using Discovery Studio Client 2018 suite of package (2018) and HCV GT 1a structure (PDB code: 1R7G) as a template (Penin et al., 2004). The modeled open and closed forms of NS5A structures were generated using the protein preparation wizard (Sastray et al., 2013) of the maestro utility in Schrödinger 2017-4 suites package [Schrödinger Release 2017-4: LLC, New York, NY 2017] at the default setting. Chemical structures of the ligands were sketched using ChemDraw Professional 16 and imported to the maestro Ligprep module. The ligand models were generated at the default setting of Ligprep module and saved as SDF format. Binding site information was obtained from previous reports, in which L31 and Y93 were mentioned as sites for drug-resistant mutations (Sorbo et al., 2018). Subsequently, the grid was assigned at the geometric center of residues L31 and Y93 of both chains of NS5A in open and closed form models. Grid expansion by 8 Å in the XYZ direction was executed to fit the ligand inside the pocket. Standard precision (SP) docking algorithm implemented inside the GLIDE docking module (Friesner et al., 2004) was used for further docking study of compounds inside the NS5A models. Fifty docking solutions were generated for each ligand and ranked according to more negative glide docking score. Tighter ligand binding inside the protein was reflected by negative glide docking score. All figures were rendered using Discovery Studio Client 2018 and Pymol 2.2.0 (<http://www.pymol.org>)



**Table 2**  
Effects of core structure of fluorene compounds on various HCV replicons.

No.	R	EC <sub>50</sub> (nM) <sup>a</sup>						CC <sub>50</sub> <sup>b</sup>
		GT 1b (NK5.1)	GT 2a (JC1)	GT 3a (S52)	GT 1b L31V	GT 1b Y93H	GT 1b L31V+Y93H	
1		0.071 ± 0.015	0.70 ± 0.05	0.336 ± 0.019	0.200 ± 0.101	18.30 ± 0.01	> 100	> 20,000
2		0.138 ± 0.037	14.5 ± 1.50	0.311 ± 0.161	0.148 ± 0.015	4.60 ± 1.60	> 100	> 20,000
3		0.002 ± 0.001	1.24 ± 0.20	0.016 ± 0.008	0.004 ± 0.000	0.88 ± 0.11	41.4 ± 29.5	> 20,000
4		0.003 ± 0.000	5.90 ± 4.90	0.007 ± 0.006	0.002 ± 0.002	2.30 ± 0.30	47.8 ± 32.7	> 20,000

<sup>a</sup> The values depict mean and standard deviation. EC<sub>50</sub>, Effective concentration 50%.

<sup>b</sup> CC<sub>50</sub>, Cytotoxicity concentration 50%. Results from three independent experiments in duplicate.

visualization tools.











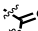





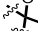

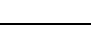
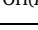
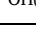
### 3. Results

#### 3.1. Effects of core structure of fluorene compounds on HCV replication

To determine the EC<sub>50</sub> of compounds on HCV replication, HCV cell culture (HCVcc) and HCV replicon systems were used (Fig. 1A) as described in materials and methods (Blight et al., 2000; Kim et al., 2011; Krieger et al., 2001; Lohmann et al., 1999; Pietschmann et al., 2006; Saeed et al., 2012). In order to improve properties of compound **43** (Table 1), which were reported previously (Bae et al., 2015), we modified residues at positions R, Y, and Z (Fig. 1B). First, we investigated the effect of alkyl chain length at the C9 position of the fluorene core (R) on HCV GTs 1b (NK5.1), 2a (JC1), and 3a (S52). In this study, we used the same linker (L-proline) and cap region (N-methoxycarbonyl phenylglycine) of the compounds (Fig. 1B). As the length of alkyl chain at the C9 position increased, the inhibitory effects of compounds on HCV GT 1b and 3a gradually increased. For compound **4**, the EC<sub>50</sub> value reached 3–7 pM range (Table 2). However, the length of alkyl chain did not linearly correlate with the EC<sub>50</sub> value of HCV GT 2a (Table 2).

Moreover, we tested the effects of compounds on HCV GT 1b containing the major daclatasvir-resistant variants such as L31V (single mutant), Y93H (single mutant), and L31V+Y93H (double mutant). Efficacy of the compounds on RAVs gradually increased as the length of the alkyl chain increased, reaching maximal effectiveness with compound **3**, which contains a 4-carbon chain (Table 3). As a result, compounds containing 9,9-dibutylfluorene and 9,9-dipentylfluorene (compounds **3** and **4**, respectively) showed very strong inhibitory effects on wild type and RAV L31V of GT 1b HCV (Table 2).

**Table 3**  
Effects of the proline structure of fluorene compounds with 9,9-dibutylfluorene core on various HCV replicons.

No.	R	Y	Z	EC <sub>50</sub> (nM) <sup>a</sup>						CC <sub>50</sub> <sup>b</sup>
				GT 1b (NK5.1)	GT 2a (JC1)	GT 3a (S52)	GT 1b L31V	GT 1b Y93H	GT 1b L31V+Y93H	
3				0.002 ± 0.000	1.2 ± 0.2	0.016 ± 0.007	0.003 ± 0.0002	0.88 ± 0.10	41.4 ± 29.5	> 20,000
5				0.004 ± 0.000	0.73 ± 0.07	0.029 ± 0.012	0.004 ± 0.001	0.78 ± 0.10	14.8 ± 6.6	> 20,000
6				0.006 ± 0.001	1.6 ± 0.4	0.030 ± 0.004	0.007 ± 0.007	0.08 ± 0.03	1.04 ± 0.1	> 20,000
7				0.014 ± 0.001	0.65 ± 0.02	0.082 ± 0.022	0.004 ± 0.001	0.15 ± 0.25	2.2 ± 0.3	> 20,000
8				0.022 ± 0.009	1.4 ± 0.6	0.079 ± 0.01	0.003 ± 0.003	0.024 ± 0.002	0.44 ± 0.06	> 20,000
9				0.005 ± 0.001	5.6 ± 0.6	0.354 ± 0.006	0.007 ± 0.002	0.045 ± 0.001	0.033 ± 0.003	> 20,000
10				0.029 ± 0.008	3.5 ± 0.12	0.133 ± 0.012	0.025 ± 0.002	0.029 ± 0.002	0.058 ± 0.002	> 20,000

<sup>a</sup> The values depict mean and standard deviation. EC<sub>50</sub>, Effective concentration 50%.

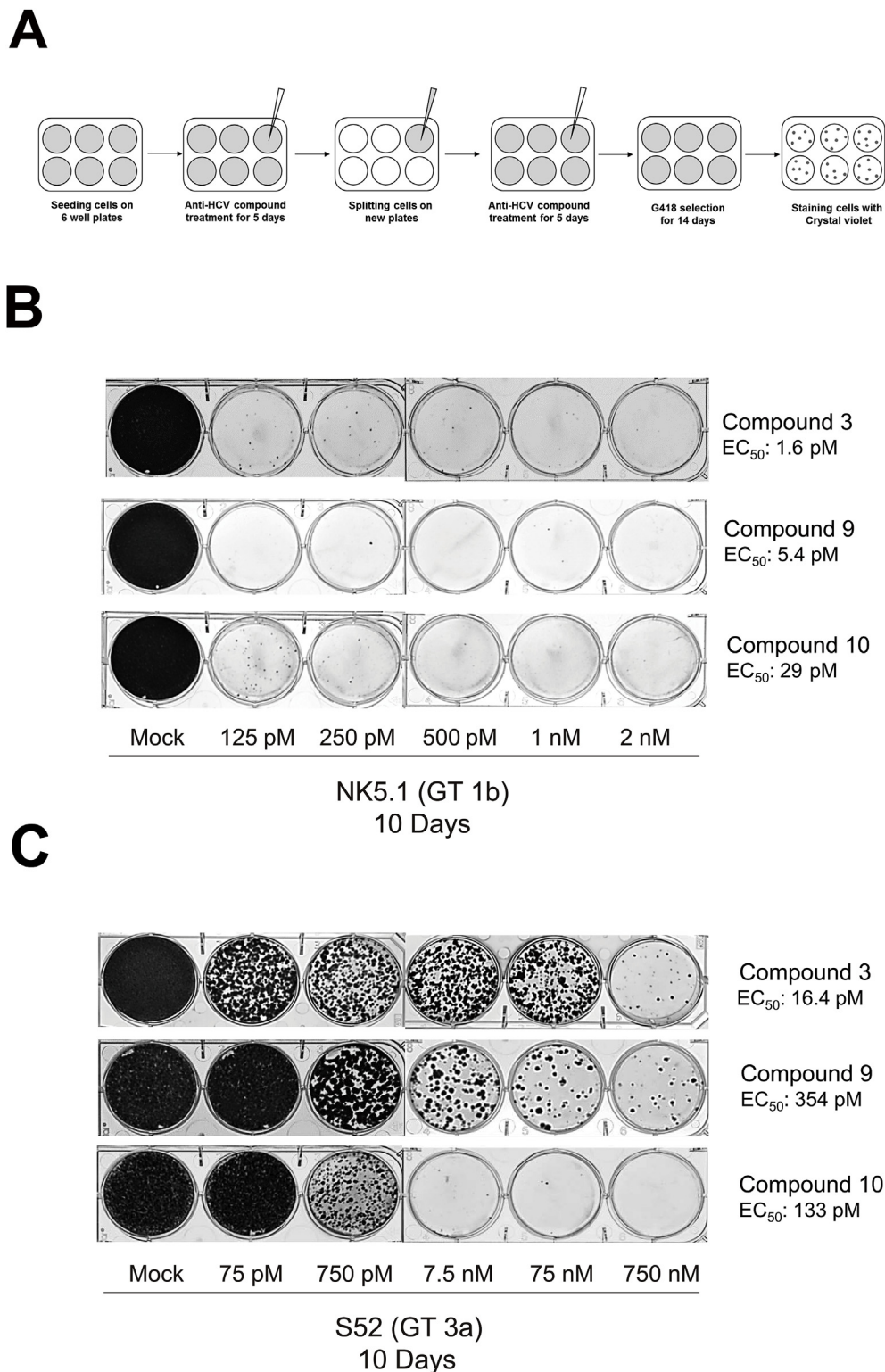
<sup>b</sup> CC<sub>50</sub>, Cytotoxicity concentration 50%. Results from three independent experiments in duplicate.

#### 3.2. Effects of the proline structure of fluorene compounds on HCV replication

To investigate the effect of proline residues of compounds **3**, we fixed the core residue with 9,9-dibutylfluorene (Table 3) and assessed the effect of the C4 position of L-proline residues (Fig. 1B, Y and Z positions) on various GTs of HCV and RAVs of GT 1b. As shown in Table 2, the parental compound (compound **3**) showed very strong anti-HCV effects against GT 1b and GT 3a, but weak effects against GT 2a (Table 3). Moreover, compounds **3** and **4** were very effective on RAV L31V of GT 1b, but not highly effective against both RAVs Y93H and L31V+Y93H (Table 2). Interestingly, modifications of the C4 position of proline residues (Y and Z positions in Fig. 1B) showed dramatic effects on RAVs Y93H and L31V+Y93H (Table 3 and Table S1). Particularly, substitutions of proline to 4-spirocyclic ketal-L-proline (compounds **6**, **8**, and **9**) or 4-hydroxyl-L-proline (compound **10**) improved the efficacies of compounds against RAVs Y93H and L31V+Y93H (Table 3).

#### 3.3. Selection of RAVs after anti-HCV compound treatment

We investigated genetic resistance barriers of compounds by measuring colony-forming efficiencies of Huh7.5.1 cells containing the GT 1b or GT 3a replicon after anti-HCV compound treatments at various concentrations for 10 days (Fig. 2A) (Wang et al., 2012). After compound treatments, the cells were split in new plates and treated with G418 (1 mg/ml) for 14 days in the absence of anti-HCV compound to select replicon-containing cells. The cell colonies were visualized by Crystal violet staining (Fig. 2A) or maintained for additional investigations. We performed colony-forming assays with compounds **3**, **9**, **10**, and reference compounds using replicons GT 1b (Fig. 2B, Fig. S2A) and GT 3a (Fig. 2C, Fig. S2B). All of the compounds, including the



**Fig. 2. Effects of fluorene compounds on colony formations of Huh 7.5.1 cells containing subgenomic replicons.** (A) Schematic diagram of colony formation assay. Colony formation assays were performed as described in Materials and Methods. (B) Effects of compounds **3**, **9**, and **10** on the colony formation of Huh 7.5.1 cells containing the GT 1b replicon NK5.1-Gluc. (C) Effects of compounds **3**, **9**, and **10** on the colony formation of Huh 7.5.1 cells containing the GT 3a replicon S52-Feo.

reference inhibitors (daclatasvir and velpatasvir), showed higher efficacy to GT 1b than GT 3a, which was indicated by the number of colonies after compound treatments and EC<sub>50</sub> values (compare Fig. 2B with 2C, and S2A with S2B). Treatments of compounds **9** and **10** for 10 days completely inhibited colony formation of Huh7.5.1 cells

containing a GT 1b replicon at 500 pM or higher concentrations (Fig. 2B). Interestingly, compound **3** showed a higher inhibitory effect than compound **10** against GT 3a at a low concentration (75 pM); however, compound **10** showed higher inhibitory effect than compound **3** at high concentrations (7.5 nM or higher) in drug-resistant colony-

forming assays (Fig. 2C, also see below).

### 3.4. Mutations in RAVs selected during inhibitor treatments

We analyzed mutations in the HCV replicon RNAs (GT 3a) that were selected during treatments of inhibitors targeting NS5A. We used different concentrations of inhibitors [compounds **3** (750 pM and 750 nM) and **10** (75 pM and 750 pM), daclatasvir (75 nM), and velpatasvir (7.5 nM)] since each compound has different upper concentration limit allowing colony formation (Fig. 2, Fig. S2). We used the selection concentrations near the upper limits of individual compounds producing enough colonies to identify various mutations that provided strong resistance against the compounds.

As reported previously (Fridell et al., 2010; Lawitz et al., 2016), either substitution of tyrosine to histidine at amino acid 93 (Y93H) or substitution of leucine to valine at amino acid 31 (L31V) in NS5A was the major mutations providing resistance against daclatasvir or velpatasvir, respectively (Fig. S3). Several other mutations in various parts of NS5A domain 1 were also observed in most of RAVs (Fig. S3). Double mutation at L31 and Y93 was not found in velpatasvir-treated cells, and the double mutation [Y93H and substitution of leucine to phenylalanine at amino acid 93 (L31F)] was found only once in daclatasvir-treated cells. In contrast, the major RAVs of HCV replicons in compound **3** (750 pM)-treated cells contained substitutions of both L31V and Y93H (Fig. 3A). Moreover, most of the RAVs had an additional substitution of methionine to threonine at amino acid 79 (M79T) in NS5A. One of the RAVs had a substitution of leucine to phenylalanine at amino acid 31 (L31F) and an additional substitution of threonine to isoleucine (T95I) instead of L31V, Y93H, and M79T mutations in NS5A (Fig. 3A). Furthermore, all RAVs of HCV replicons selected at higher concentration of compound **3** (750 nM) contained Y93H substitution. One or two additional mutations (A25T, L74R, and L31V + M79T) were observed in all RAVs selected at 750 nM of compound **3** (Fig. S4A). The results indicated that Y93H substitution is the key mutation providing resistance against compound **3**, and that additional mutations are required for strong resistance against compound **3** at high concentration. Interestingly, L31V and L31F substitutions were the dominating mutations of RAVs selected by treatment of compound **10** (75 pM or 750 pM) (Fig. S4B, Fig. 3B, respectively). Occasionally, however, substitution of threonine to alanine at amino acid 21 (T21A) and substitution of lysine to arginine at amino acid 20 (K20R), both of which reside in the amphipathic helix close to the leucine 31, were observed in RAVs selected by compound **10** at 75 pM (Fig. S4B). No Y93H substitution was observed from the RAVs selected by compound **10** at 75 pM (Fig. S4B). However, Y93H substitution was found in a few RAVs selected by compound **10** at 750 pM (Fig. 3B). The results indicated that substitutions in or around the amphipathic helix are the main mutations providing resistance against compound **10**.

Through the analyses of the RAVs, we conjectured that the mutations contributing to resistances to different compounds varies significantly even though the sites of frequent mutations are generally fixed. This might indicate that a specific mutation(s) providing strong resistance to a specific compound might not significantly affect the susceptibility to a compound with a high genetic barrier for RAV development. Indeed, the pools of replicon containing cells (GT 3a) selected by either daclatasvir (75 nM) or velpatasvir (7.5 nM) were highly susceptible to compound **10** ( $EC_{50}$ s were 0.58 nM and 0.74 nM, respectively) (Fig. 3C). The results were consistent with the higher difficulties of GT 3a RAV generations by compound **10** than those by daclatasvir and velpatasvir (compare Fig. 2C with Fig. S2).

Effects of co-treatment of grazoprevir (a NS3/4A proteinase inhibitor) and fluorene compounds on HCV replication.

We further analyzed compound **10** containing 4-hydroxyl-L-proline and compound **3** containing unmodified L-proline since compound **10** showed the highest genetic resistance barrier for GT 3a and strong inhibitory effects against both GT 1b and GT 3a. The effects of co-

treatment of these compounds with grazoprevir were investigated since standard anti-HCV therapy includes two or more drugs to minimize RAV generation.  $EC_{90}$  concentrations of grazoprevir (2 nM and 100 nM for GT 1b and GT 3a, respectively) were used in combination with the indicated amounts of anti-NS5A compounds for 10 days. Huh7.5.1 cells containing drug-resistant replicons were selected by G418 treatment. Single treatments of 2 nM and 100 nM of grazoprevir on GT 1b and GT 3a, respectively, resulted in significant cell growth (top panel in Fig. 4A and 4B). In contrast, no colony formation was observed from GT 1b replicon-containing cells treated with 2 nM of grazoprevir together with 125 pM (or higher concentration) of compounds **3** and **10**. The data indicated that compounds **3** and **10** were very effective against GT 1b when co-treated with grazoprevir.

Co-treatment of grazoprevir with compounds **3** and **10** showed various antiviral activities against the GT 3a replicon. No colony formation was observed with 100 nM of grazoprevir ( $EC_{90}$  value) and 75 pM of compound **3** or 750 pM of compound **10** (Fig. 4B) co-treatment. Further, co-treatment of grazoprevir with compound **3** eliminated colony formation at lower concentration than that with compound **10** (Fig. 4B). This effect is likely attributed to the lower  $EC_{50}$  value of compound **3** than compound **10** against GT 3a (Table 3). These data indicated that co-treatment of anti-NS3/4A (grazoprevir) and anti-NS5A compounds was much more effective than mono-treatment of either anti-NS3A/4A or anti-NS5A compounds (Fig. 2B) for complete elimination of HCV RNA in cells.

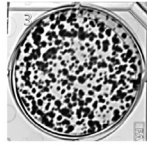
To characterize co-treatment effects, we calculated combination index (CI) values using the Compusyn freeware program (Compusyn, Inc.) (Chou and Martin, 2005). Huh7.5.1 cells containing either GT 1b or GT 3a were co-treated with grazoprevir and compounds **3**, **9** and **10**, and CI values were calculated (Table 4). The CI values of compounds at  $EC_{50}$  and  $EC_{75}$  were less than or equal to 1. The results indicated that the co-treatment effects were either synergic or additive. These synergistic and additive effects likely attributed to the two different mechanisms of actions (proteinase inhibition and replication inhibition) executed against the two distinct target molecules (NS3/4A and NS5A, respectively) in the compound co-treatments.

### 3.5. Molecular docking analysis

We performed molecular docking analyses using the models of NS5A domain I, open model (1ZH1-based model) (Tellinghuisen et al., 2005) and closed-model (3FQQ-based model) (Love et al., 2009), including the N-terminal amphipathic helix. To understand why compound **10** had a stronger anti-viral effect than compound **3** against GT 1b HCV containing double mutations in NS5A, we analyzed the docking models of compounds **3** and **10** inside the closed form of dimeric GT 1b HCV NS5A (A/B) containing the double mutant (L31V/Y93H).

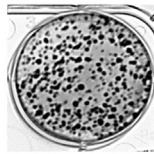
Figure S5A represents the docked model of compound **3** inside closed-model (glide docking score =  $-6.26$  kcal/mol) (Love et al., 2009). 9,9-dibutyl-9H-fluorene core of compound **3** interacted with the binding pocket residues (A:Cys57, A:Gly60, A:Ala61, A:ILE63, B:Thr56, B:Ala61) of NS5A through van der Waals interaction. Val31 of subunit A showed pi-alkyl interaction with one of the proline ring and alkyl-alkyl interaction with terminal methyl of ester moiety. His93 of subunit A showed pi-alkyl and hydrogen bond interactions with methyl group of ester and carbonyl oxygen of ester, respectively. Val31 of subunit B showed pi-alkyl interaction with the phenyl of other end of compound **3**. Ester amide 'NH' showed hydrogen bond interaction with Gln62 of subunit A. Side chain of Gln54 in subunit A interacted via two hydrogen bonds with proline amide 'O' and 'NH' of amide linker which connected central core and proline. Ile63 of subunit A interacted with n-butyl on central core, and His93 of subunit B interacted with the central core and proline amide via van der Waals interaction.

Figure S5B represents the docked model of compound **10** inside closed-model (glide docking score =  $-7.04$  kcal/mol) (Love et al., 2009). *n*-Butyl moiety at the central core of compound **10** interacted

**A**

Number of clone	Mutations in GT 3a HCV resistant to Compound 3 (750 $\mu$ M)			
	L31	M79	Y93	Other mutations
9	L31V	M79T	Y93H	-
1	L31V	M79T	Y93H	A75V
1	L31V	M79T	Y93H	I63T
1	L31F	-	-	T95I
Total	12			

-: No mutation

**B**

Number of clone	Mutations in GT 3a HCV resistant to Compound 10 (750 $\mu$ M)		
	L31	Y93	Other mutations
1	L31F	-	F19I, L23H
2	L31F	-	F19I, L23H, A25T
1	L31F	-	T94A
1	-	Y93H	A25T, F36S
1	L31F	-	N82I
1	-	Y93H	-
1	L31F	-	-
1	L31F	-	G33R, R73W
Total	9		

-: No mutation

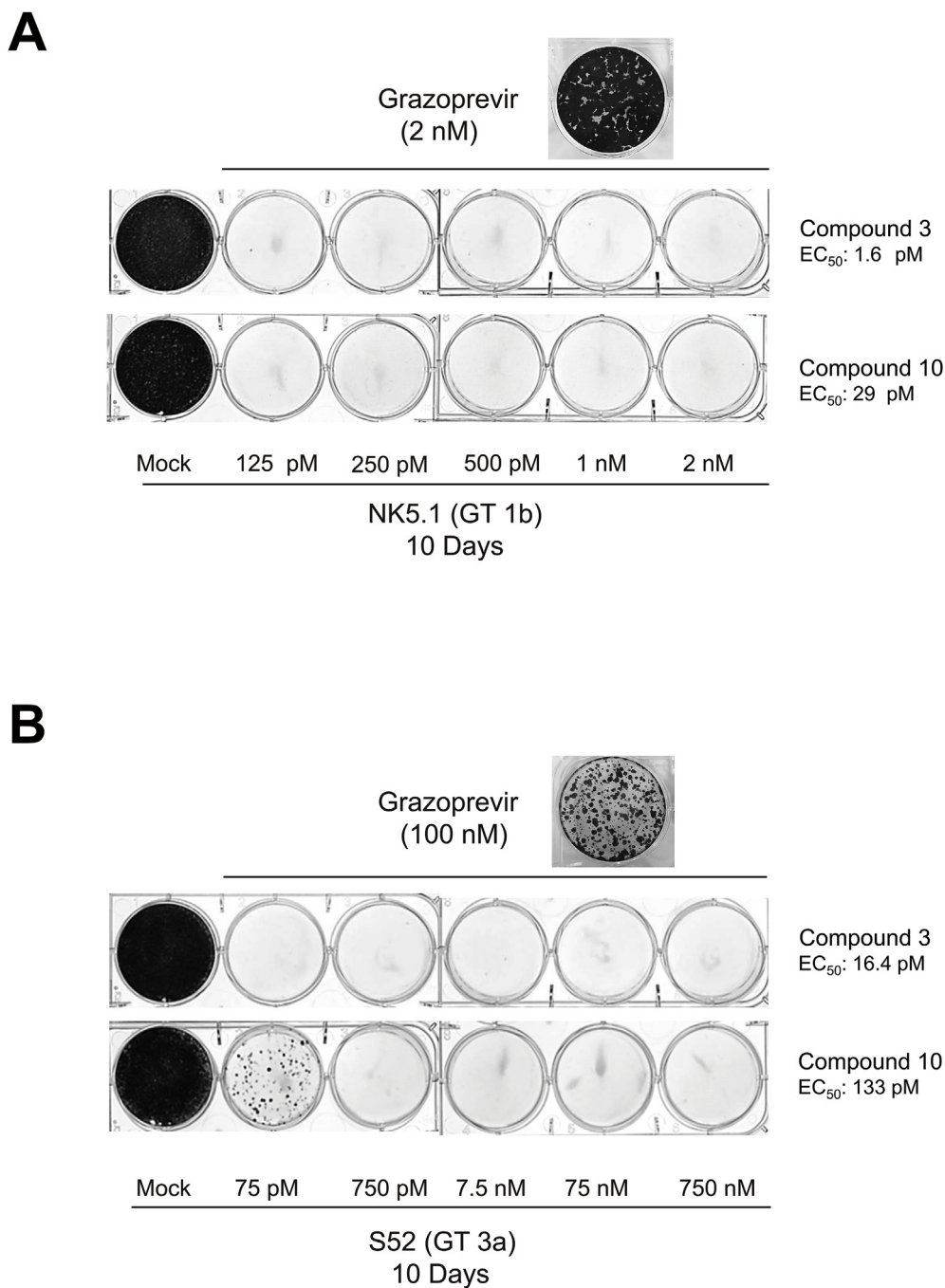
**C**

GT 3a	EC <sub>50</sub> (nM)	
	DCV-resistant replicon (75 nM)	VEV-resistant replicon (7.5 nM)
Velpatasvir	20.1 $\pm$ 1.1	14.3 $\pm$ 3.3
Compound 10	0.76 $\pm$ 0.3	0.74 $\pm$ 0.1

DCV: Daclatasvir; VEV: Velpatasvir

**Fig. 3. Mutations in RAVs selected during inhibitor treatments.** (A) Mutations in replicon GT 3a selected during treatment of compound 3 at 750  $\mu$ M. (B) Mutations in replicon GT 3a selected during treatment of compound 10 at 750  $\mu$ M. (C) EC<sub>50</sub> values of velpatasvir and compound 10 on pools of GT 3a replicon-containing cells selected by treatment of daclatasvir (75 nM) or velpatasvir (7.5 nM).





**Fig. 4. Effects of co-treatment of grazoprevir and fluorene compounds on colony formations of Huh 7.5.1 cells containing subgenomic replicons. (A)** Effects of co-treatment of grazoprevir (EC<sub>90</sub> = 2 nM) and compound 3 and 10 on the colony formation of Huh 7.5.1 cells containing a GT 1b replicon NK5.1-Gluc. **(B)** Effects of co-treatment of grazoprevir (EC<sub>90</sub> = 100 nM) and compound 3 and 10 on the colony formation of Huh 7.5.1 cells containing a GT 3a replicon S52-Feo.

**Table 4**  
CI values of compounds with Grazoprevir (a NS3/4A inhibitor).

Compound	Combination	EC <sub>50</sub> CI value <sup>a, b</sup>		EC <sub>75</sub> CI value <sup>a, c</sup>	
		GT 1b (NK5.1)	GT 3a (S52)	GT 1b (NK5.1)	GT 3a (S52)
3	Grazoprevir	0.8 ± 0.04	0.6 ± 0.30	1.0 ± 0.13	0.8 ± 0.32
9	Grazoprevir	0.7 ± 0.17	0.6 ± 0.09	0.9 ± 0.18	0.7 ± 0.04
10	Grazoprevir	0.7 ± 0.09	1.0 ± 0.05	0.9 ± 0.12	0.9 ± 0.01

CI > 1, Antagonistic effect; CI < 1, Synergistic effect; CI = 1, Additive effect. Results from three independent experiments in duplicate.

<sup>a</sup> The values depict mean and standard deviation.

<sup>b</sup> EC<sub>50</sub> CI value, Effective concentration 50 percent combination index value.

<sup>c</sup> EC<sub>75</sub> CI value, Effective concentration 75 percent combination index value.

with Ala61 of subunit A via alkyl-alkyl and with A:Thr55, A:Gly60, A:Ile63, A:Thr95, B:Thr56, B:Gly60, and B:Ala61 via van der Waals interactions. The 4-hydroxyl-L-proline moiety of compound **10** interacted with A: Cys57 and B: His93 of NS5A via two hydrogen bonds.

The areas in NS5A interacting with inhibitors were predicted to be similar to those predicted by previous docking study of daclatasvir inside closed-model (Love et al., 2009) that suggested residues Leu31, Pro32, Val34, Ile52, Gln54, Thr56, Gly60, Gln62, Tyr93, Thr95, and Pro97 participated in complex formation with the inhibitor (Ascher et al., 2014). However, the detailed residues and chemical bonds contributing to the protein-inhibitor interactions differed from each other.

Through the molecular docking analyses we found that the closed model fitted better than the open model in terms of the relationship between predicted affinity and inhibitor efficacy and the effects of inhibitors on the double mutant HCV (see below).

#### 4. Discussion

Over the last several years, remarkable progress has been made in the development of DAAs against HCV, and several anti-HCV drugs are currently available (Grebely et al., 2017; Zhang et al., 2016). However, the uneven efficacies of drugs against various GTs of HCV and the spontaneous generation of RAVs remain as unsolved issues in HCV therapeutics (Raj et al., 2017). HCV has an error-prone RNA-dependent RNA polymerase (RdRp) NS5B, which shows no proofreading activity during the RNA polymerization reaction (Poch et al., 1989). Therefore, HCV variants (quasispecies) can quickly generate following HCV cultivation for several generations, even if they originated from a single clone. Upon anti-HCV compound treatment, compound-sensitive HCV variants are unable to replicate. However, drug-resistant variants existing in a minor proportion replicate continuously, even in the presence of an anti-HCV drug, and quickly expand to large populations. The genetic resistance barrier of a particular compound can be monitored by measuring the colony-forming efficiency of replicon-containing cells in the presence of the compound (Wang et al., 2012). For example, Huh7.5.1 cells containing a variant of HCV replicon resistant to an anti-HCV compound will grow even in the presence of the compound and Geneticin (G418) since HCV replicon RNAs contain the neomycin-resistance gene (Neo<sup>R</sup> in Fig. 1A).

Efforts have been made to create new NS5A inhibitors for anti-HCV drug therapy. Previously, we reported highly effective fluorene compounds against GT 1b. To improve the efficacy of compounds against GT 3 and RAVs of HCV GT 1b, we modified residues at the R, Y, and Z positions of compound **43** that was reported previously (Bae et al., 2015) (Fig. 1B). The length of alkyl chains at the C9 of fluorene (R position) affected the anti-HCV activity of compounds to GT 1b, GT 3a, and RAVs of GT 1b. Compounds containing 9,9-dibutylfluorene and 9,9-dipentylfluorene cores (compounds **3** and **4**, respectively) showed very strong inhibitory effects against wild type GT 1b, wild type GT 3a, and RAVs L31V of GT 1b (Table 2). We further modified the compounds **3** and **4** to improve anti-HCV effects. In this study, we focused on the L-proline residues of compounds (Y and Z positions in Fig. 1B) since L-proline substitutions with 4-oxo-L-proline (Bae et al., 2015) or 4-spirocyclic ketal-L-proline (Kazmierski et al., 2014) improved anti-viral effects against wild type HCV or RAVs, respectively (Table 3 and S1). Particularly, substitutions of L-proline to 4-spirocyclic ketal-L-proline (compounds **6**, **8**, **9**, **12**, **14**, and **15**) or 4-hydroxyl-L-proline (compound **10**) improved the efficacy of compounds against RAVs Y93H and L31 + Y93H (Table 3 and S1). These results suggest that the L-proline residues of compounds may localize in the vicinity of residue 93 (Y93) of NS5A and that both 4-spirocyclic ketal-L-proline and 4-hydroxyl-L-proline may allow binding of compounds to the histidine at residue 93.

The colony-forming efficiencies of Huh7.5.1 cells containing a GT 3a replicon showed peculiar patterns after anti-HCV compound treatment. Compound **3** showed higher inhibitory effects than compound **10** in drug-resistant colony formation assays at low concentrations (75

pM). In contrast, compound **10** showed higher inhibitory effects at high concentrations (7.5 nM or higher) (Fig. 2C). The higher efficacy of compound **3** at low concentrations is likely attributed to the lower EC<sub>50</sub> value of compound **3** than compound **10** (16 pM vs. 133 pM in Table 3). Further, the higher efficiency of compound **10** at the high concentration is likely attributed to the higher activity of compound **10** against RAVs, such as Y93H and L31V + Y93H. These data clearly demonstrate that the general efficacy of a compound (EC<sub>50</sub>) differs from the genetic resistance barrier of the compound. As such, compound **3** is more effective than compound **10** against wild types of GT 1b and GT 3a; yet, the genetic resistance barrier of compound **10** is higher than compound **3** against GT 3a. Importantly, the genetic resistance barrier of compound **10** is higher than velpatasvir, which is a second generation NS5A inhibitor, against GT 3a (compare Fig. 2C with Fig. S2B).

Moreover, compound **10** effectively inhibited a pool of GT 3a replicons which were selected by treatment of velpatasvir (7.5 nM). The EC<sub>50</sub>'s of compound **10** and velpatasvir against these GT 3a RAVs were 0.74 and 14.3 nM, respectively (Fig. 3C). Compounds possessing high genetic resistance barriers such as compound **10** are good candidates for developing an anti-HCV drug for patients who were not successfully treated with currently available drugs.

To minimize the RAV issue of anti-HCV drugs, combined treatment with compounds having different mechanisms of action and different target molecules is recommended (Polish Group of Experts for et al., 2017). In this regard, we observed synergistic and/or additive effects of anti-NS5A compounds (compounds **3**, **9**, and **10**) with grazoprevir (NS3/NS4A proteinase inhibitor) (Fig. 4). In practical applications, however, co-treatment of compound **10** and another NS3/4A inhibitor is recommendable for treatment of GT 3a since grazoprevir is not recommended for treating GT 3a (Sulejmani and Jafri, 2018).

We performed molecular docking analyses using the models of the NS5A domain I, including the N-terminal amphipathic helix, to understand the molecular bases of anti-HCV activities of compounds **3** and **10**, and the higher efficacy of compound **10** relative to compound **3** to RAVs. Experimental results fitted better with the closed-model (3FQQ-based model) (Tellinghuisen et al., 2005) than the open model (1ZH1-based model) (Love et al., 2009). In general, predicted binding affinities of inhibitors (compounds **3**, **10**) to wild type HCV were higher than to double mutant HCV when the closed model was used (Fig. S5C). These results correlate well with higher efficacies of these compounds to wild type than to mutant HCV (Table 3). Moreover, the rank of predicted affinities of inhibitors to double mutants fitted well with the rank of efficacies of inhibitors to mutant HCV when the closed model was used (Table 3 and Fig. S5C). However, the relationship between predicted affinity and inhibitory efficacy did not match well with wild type HCV, which is extremely sensitive to the compounds. This may indicate that the affinity prediction by the molecular docking is useful for rough estimation of efficacies of compounds with a wide range of efficacy (58 pM–41 nM), but not so useful for precise efficacy estimation of compounds with subtle difference in efficacies (2–29 pM). The limitation of affinity predictability of the molecular docking is likely attributed, at least in part, to the uncertainty of the real structure of NS5A.

Addition of 4-hydroxyl group at the C4-position of L-proline (compound **10**) resulted in much stronger anti-viral activity than that of unmodified L-proline (compound **3**) against double mutant GT 1b (EC<sub>50</sub> = 58 pM vs. 41 nM). According to the molecular docking analysis, compounds **10** and **3** had glide docking scores of −7.04 kcal/mol and −6.26 kcal/mol, respectively. Two more hydrogen bonds to the double mutant were possible for compound **10** compared with compound **3**. One of them was a hydrogen bond between the hydroxyl group at the C4 position of L-proline and histidine 93, a resistance-associated substitution, which is depicted by a red circle in Fig. S5B. These additional interactions likely contribute to the strong inhibitor binding and high activity of compound **10** to double mutant HCV.

In conclusion, we developed NS5A inhibitors containing a fluorene proline-amide skeleton and the structure-activity relationships of the

compounds were analyzed. Moreover, we investigated the molecular bases of the inhibitory activities of some compounds by the molecular docking method. Through these approaches, we developed a compound (designated as compound 10) that is very effective against GT 1b, GT 3, and RAVs of GT 1b. This compound showed no cytotoxicity, very low drug-drug interaction issues (determined by CYP inhibition test), and no cardiotoxicity (determined by hERG ligand binding assays) (Tables S2 and S3). Further investigations are in progress to improve the physicochemical property of compound 10.

## Acknowledgement

GT 3a replicon clone (S53-Feo) was kindly provided by Dr. Charles M. Rice (The Rockefeller University). This research was supported by the Bio & Medical Technology Development Program of the National Research Foundation (NRF) funded by the Ministry of Science and ICT (NO. NRF-2017M3A9F6029755).

## Appendix A. Supplementary data

Supplementary data to this article can be found online at <https://doi.org/10.1016/j.antiviral.2019.104678>.

## Abbreviations

HCV	Hepatitis C virus
DAA	direct-acting antiviral
SVR	sustained virologic response
Peg-IFN $\alpha$	pegylated interferon $\alpha$
NS5A	hepatitis C virus nonstructural protein 5A
pM	Picomolar
nM	Nanomolar
EC <sub>50</sub>	Effective concentration 50%
CC <sub>50</sub>	cytotoxic concentration 50%

## References

- Kim, Hee Sun, Y. Y., Bae, Il Hak, Mun, Jae Gon, Hee Jo Moon Byeong Moon Kim, Sung Key Jang, March, 2019. In: Fluorene Derivative or Pharmaceutically Acceptable Salt Thereof, Preparation Method Thereof, and Pharmaceutical Composition Comprising Same as Effective Ingredient for Preventing or Treating Hcv-Related Disease, WO2019059687A1.
- Ascher, D.B., Wielens, J., Nero, T.L., Doughty, L., Morton, C.J., Parker, M.W., 2014. Potent hepatitis C inhibitors bind directly to NS5A and reduce its affinity for RNA. *Sci. Rep.* 4, 4765.
- Badillo, A., Receveur-Brechot, V., Sarrazin, S., Cantrelle, F.-X., Delolme, F., Fogeron, M.-L., Molle, J., Montserret, R., Bockmann, A., Bartenschlager, R., Lohmann, V., Lippens, G., Ricard-Blum, S., Hanouille, X., Penin, F., 2017. Overall structural model of NS5A protein from hepatitis C virus and modulation by mutations conferring resistance of virus replication to cyclosporin A. *Biochemistry* 56, 3029–3048.
- Bae, I.H., Kim, H.S., You, Y., Chough, C., Choe, W., Seon, M.K., Lee, S.G., Keum, G., Jang, S.K., Kim, B.M., 2015. Novel benzidine and diamino fluorene prolinamide derivatives as potent hepatitis C virus NS5A inhibitors. *Eur. J. Med. Chem.* 101, 163–178.
- Blight, K.J., Kolykhalov, A.A., Rice, C.M., 2000. Efficient initiation of HCV RNA replication in cell culture. *Science* 290, 1972–1974.
- Chou, T., Martin, N., 2005. CompuSyn for Drug Combinations and for General Dose-Effect Analysis, Software and User's Guide: A Computer Program for Quantitation of Synergism and Antagonism in Drug Combinations, and the Determination of IC50 and ED50 and LD50 Values. ComboSyn Inc, Paramus, NJ, USA.
- Dassault Systems BIOVIA, 2018. Discovery Studio Modeling Environment, Release 2018. Dassault Systèmes, San Diego 2018.
- Fridell, R.A., Qiu, D.K., Wang, C.F., Valera, L., Gao, M., 2010. Resistance analysis of the hepatitis C virus NS5A inhibitor BMS-790052 in an in vitro replicon system. *Antimicrob. Agents Chemother.* 54, 3641–3650.
- Friesner, R.A., Banks, J.L., Murphy, R.B., Halgren, T.A., Klicic, J.J., Mainz, D.T., Repasky, M.P., Knoll, E.H., Shelley, M., Perry, J.K., Shaw, D.E., Francis, P., Shenkin, P.S., 2004. Glide: a new approach for rapid, accurate docking and scoring. 1. Method and assessment of docking accuracy. *J. Med. Chem.* 47, 1739–1749.
- Grebely, J., Hajarizadeh, B., Dore, G., 2017. Direct-Acting antiviral agents for HCV infection affecting people who inject drugs. *Nat. Rev. Gastroenterol. Hepatol.* 14.
- He, Y., Staschke, K.A., Tan, S.-L., 2006. HCV NS5A: a multifunctional regulator of cellular

- pathways and virus replication. *Hepat. C Viruses: Genomes Mol. Biol.* 267–292.
- Huang, Y., Staschke, K., De Francesco, R., Tan, S.-L., 2007. Phosphorylation of hepatitis C virus NS5A nonstructural protein: a new paradigm for phosphorylation-dependent viral RNA replication? *Virology* 364, 1–9.
- Kazmierski, W.M., Maynard, A., Duan, M., Baskaran, S., Botyanski, J., Crosby, R., Dickerson, S., Tallant, M., Grimes, R., Hamatake, R., Leivers, M., Roberts, C.D., Walker, J., 2014. Novel spiroketal pyrrolidine GSK2336805 potently inhibits key hepatitis C virus genotype 1b mutants: from lead to clinical compound. *J. Med. Chem.* 57, 2058–2073.
- Khullar, Vikas, Firpi, Roberto J., 2015. Hepatitis C Cirrhosis: New Perspectives for Diagnosis and Treatment, vol. 7. pp. 1843.
- Kim, C.S., Keum, S.J., Jang, S.K., 2011. Generation of a cell culture-adapted hepatitis C virus with longer half life at physiological temperature. *PLoS One* 6, e22808.
- Krieger, N., Lohmann, V., Bartenschlager, R., 2001. Enhancement of hepatitis C virus RNA replication by cell culture-adaptive mutations. *J. Virol.* 75, 4614.
- Lambert, S.M., Langley, D.R., Garnett, J.A., Angell, R., Hedgethorpe, K., Meanwell, N.A., Matthews, S.J., 2014. The crystal structure of NS5A domain 1 from genotype 1a reveals new clues to the mechanism of action for dimeric HCV inhibitors. *Protein Sci.* 23, 723–734.
- Lawitz, E.J., Dvory-Sobol, H., Doehle, B.P., Worth, A.S., McNally, J., Brainard, D.M., Link, J.O., Miller, M.D., Mo, H., 2016. Clinical resistance to velpatasvir (GS-5816), a novel pan-genotypic inhibitor of the hepatitis C virus NS5A protein. *Antimicrob. Agents Chemother.* 60, 5368–5378.
- Lohmann, V., Körner, F., Koch, J.-O., Herian, U., Theilmann, L., Bartenschlager, R., 1999. Replication of subgenomic hepatitis C virus RNAs in a hepatoma cell line. *Science* 285, 110–113.
- Love, R.A., Brodsky, O., Hickey, M.J., Wells, P.A., Cronin, C.N., 2009. Crystal structure of a novel dimeric form of NS5A domain I protein from hepatitis C virus. *J. Virol.* 83, 4395–4403.
- Messina, J.P., Humphreys, I., Flaxman, A., Brown, A., Cooke, G.S., Pybus, O.G., Barnes, E., 2015. Global distribution and prevalence of hepatitis C virus genotypes. *Hepatology* 61, 77–87.
- Penin, F., Brass, V., Appel, N., Ramboarina, S., Montserret, R., Ficheux, D., Blum, H.E., Bartenschlager, R., Moradpour, D., 2004. Structure and function of the membrane anchor domain of hepatitis C virus nonstructural protein 5A. *J. Biol. Chem.* 279, 40835–40843.
- Phan, T., Beran, R.K., Peters, C., Lorenz, I.C., Lindenbach, B.D., 2009. Hepatitis C virus NS2 protein contributes to virus particle assembly via opposing epistatic interactions with the E1-E2 glycoprotein and NS3-NS4A enzyme complexes. *J. Virol.* 83, 8379–8395.
- Pietschmann, T., Brown, R.J.P., 2019. Hepatitis C virus. *Trends Microbiol.* 27, 379–380.
- Pietschmann, T., Kaul, A., Koutsoudakis, G., Shavinskaya, A., Kallis, S., Steinmann, E., Abid, K., Negro, F., Dreux, M., Cosset, F.L., Bartenschlager, R., 2006. Construction and characterization of infectious intragenotypic and intergenotypic hepatitis C virus chimeras. *Proc. Natl. Acad. Sci. U. S. A.* 103, 7408–7413.
- Poch, O., Sauvaget, I., Delarue, M., Tordo, N., 1989. Identification of four conserved motifs among the RNA-dependent polymerase encoding elements. *EMBO J.* 8, 3867–3874.
- Polish Group of Experts for, H.C.V., Halota, W., Flisiak, R., Juszczyk, J., Małkowski, P., Pawłowska, M., Simon, K., Tomasiewicz, K., 2017. Recommendations for the treatment of hepatitis C in 2017. *Clin. Exp. Hepatol.* 3, 47–55.
- Raj, V.S., Hundie, G.B., Schürch, A.C., Smits, S.L., Pas, S.D., Le Pogam, S., Janssen, H.L.A., de Knecht, R.J., Osterhaus, A.D.M.E., Najera, I., Boucher, C.A., Haagmans, B.L., 2017. Identification of HCV resistant variants against direct acting antivirals in plasma and liver of treatment naïve patients. *Sci. Rep.* 7, 4688.
- Saeed, M., Scheel, T.K.H., Gottwein, J.M., Marukian, S., Dustin, L.B., Bukh, J., Rice, C.M., 2012. Efficient replication of genotype 3a and 4a hepatitis C virus replicons in human hepatoma cells. *Antimicrob. Agents Chemother.* 56, 5365–5373.
- Sastry, G.M., Adzhigirey, M., Day, T., Annabhimoju, R., Sherman, W., 2013. Protein and ligand preparation: parameters, protocols, and influence on virtual screening enrichments. *J. Comput. Aided Mol. Des.* 27, 221–234.
- Sorbo, M.C., Cento, V., Di Maio, V.C., Howe, A.Y.M., Garcia, F., Perno, C.F., Ceccherini-Silberstein, F., 2018. Hepatitis C virus drug resistance associated substitutions and their clinical relevance: update 2018. *Drug Resist. Updates : Rev. Comment. Anticancer Chemother.* 37, 17–39.
- Sulejmani, N., Jafri, S.-M., 2018. Grazoprevir/elbasvir for the treatment of adults with chronic hepatitis C: a short review on the clinical evidence and place in therapy. *Hepat. Med.* 10, 33–42.
- Tellinghuisen, T.L., Marcotrigiano, J., Rice, C.M., 2005. Structure of the zinc-binding domain of an essential component of the hepatitis C virus replicase. *Nature* 435, 374.
- Teraoka, Y., Uchida, T., Imamura, M., Hiraga, N., Osawa, M., Kan, H., Saito, Y., Tsuge, M., Abe-Chayama, H., Hayes, C.N., Makokha, G.N., Aikata, H., Miki, D., Ochi, H., Ishida, Y., Tateno, C., Chayama, K., 2018. Limitations of daclatasvir/asunaprevir plus beclabuvir treatment in cases of NS5A inhibitor treatment failure. *J. Gen. Virol.* 99, 1058–1065.
- Wang, C.F., Huang, H.C., Valera, L., Sun, J.H., O'Boyle, D.R., Nower, P.T., Jia, L.L., Qiu, D.K., Huang, X., Altaf, A., Gao, M., Fridell, R.A., 2012. Hepatitis C virus RNA elimination and development of resistance in replicon cells treated with BMS-790052. *Antimicrob. Agents Chemother.* 56, 1350–1358.
- Zhang, J., Nguyen, D., Hu, K.-Q., 2016. Chronic hepatitis C virus infection: a review of current direct-acting antiviral treatment strategies. *N. Am. J. Med. Sci.* 9, 47–54.